ACTIVE FLOW CONTROL OF VORTEX ROPE IN A CONICAL DIFFUSER

Ardalan Javadi*

Department of Applied Mechanics, Chalmers University of Technology, SE-412 96, Göteborg, Sweden

Håkan Nilsson

Department of Applied Mechanics, Chalmers University of Technology, SE-412 96, Göteborg, Sweden

ABSTRACT

The vortex rope in a flow similar to 70% of Francis turbine part-load is controlled using the active jet flows injected from the runner crown. The study is undertaken with numerical modeling using hybrid RANS-LES method. The comprehensive study of Javadi and Nilsson (J. Flow, Turbulence and combustion, 2015) is considered as the base case and the effectiveness of the flow control technique used in this paper is compared with the validated numerical results presented in that study. The continuous jets with different momentum fluxes are used. The investigation shows that the pressure pulsation, turbulent structures and the size of the vortex rope decrease with the injected jet from the runner crown. Although the volume flux of the jet is about 4% of whole flow rate of the swirl generator, the momentum flux and the jet position are decisive factors in the effectiveness of the technique.

KEYWORDS

Flow control, Vortex rope, Hybrid RANS-LES

1. INTRODUCTION

A major source of loss in hydraulic machinery is the vortex rope in the draft tube of water turbines. The flow in water turbines operating at off-design conditions often contains a strong swirl which may cause vortex breakdown and pressure pulsation in the draft tube. The vortex breakdown, occurring in the draft tube as a result of swirl residual in the flow as it leaves the turbine runner and enters the draft tube throat and creates an on-axis recirculation region [1]. The control of the vortex rope and the pressure pulsation in the draft tube have been the subject of some studies [2-3]. Recently the injection of a continuous jet from the runner crown tip is studied by Tănasă et al. [4] which led to significantly reduced frequency of the pressure fluctuations. Based on available experiences, a successful approach should address the momentum deficit near the axis but not close to the wall. In this study, the continuous jets with different axial and circumferential momentum fluxes are injected from the runner crown using advanced numerical simulations.

The hybrid RANS-LES approach is well suited for internal flows with large scale coherent structures [5]. Javadi and Nilsson [1,6] comprehensively studied a wide range of turbulence models including low- and high-Reynolds eddy-viscosity, hybrid RANS-LES and LES

**Corresponding author:* Department of Applied Mechanics Chalmers University of Technology SE-412 96, Gothenburg, Sweden, phone: +46 31 772 5295, email: ardalan.javadi@chalmers.se

models in a flow which is highly similar to the 70% part-load of the Francis turbine. They concluded that the delayed detached eddy simulation (DDES) method coupled with Spalart-Allmaras turbulence model plausibly predicts the highly swirling turbulent flow in the hydraulic machinery.

In this paper, various continuous jets with different momentum fluxes are injected from the runner crown to control the size of the vortex rope, on-axis recirculation region, pressure pulsations and the turbulent structures in the draft tube. The study is performed with DDES Spalart-Allmaras (DDES-SA) turbulence model and the results are compared with the results of Javadi and Nilsson (Flow, Turbulence and Combustion, 2015) [1] without flow control.

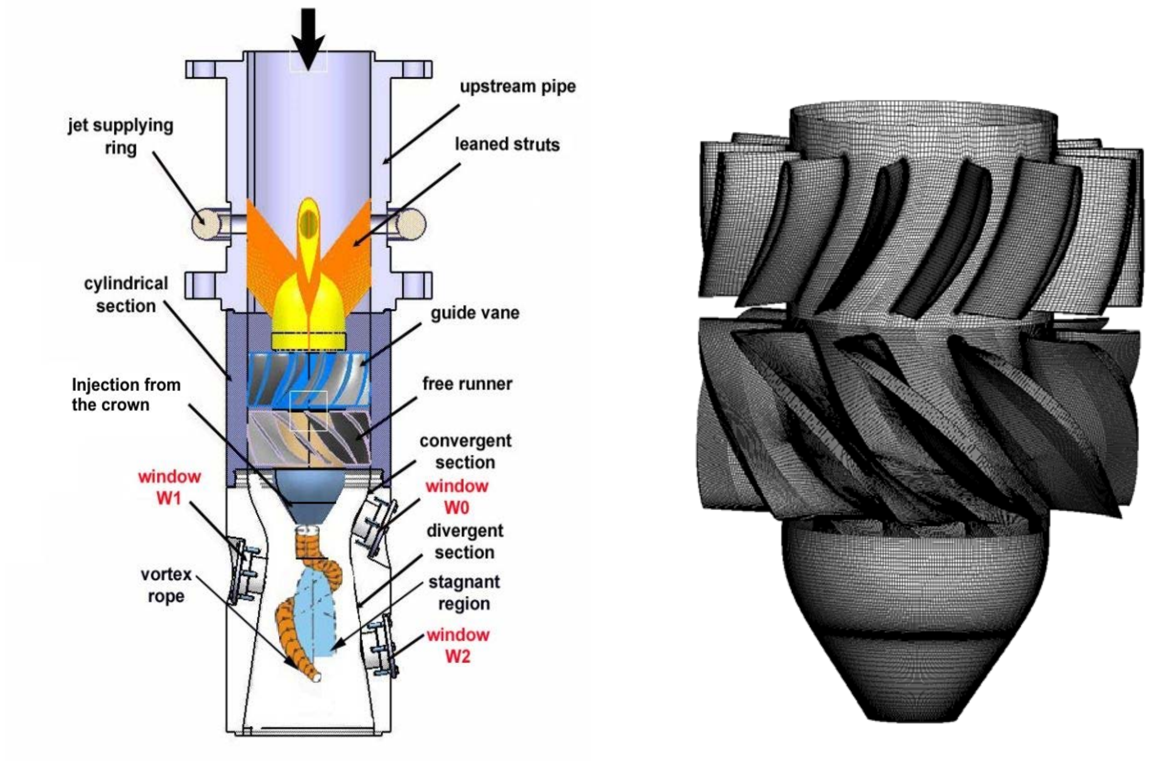

(a) *(b)*

Fig.1 (a) Schematic of swirl generator (b) mesh resolution used in simulations

2. FLOW CONFIGURATION AND COMPUTATIONAL METHOD

Figure 1 schematically shows the studied swirl generator. The experimental test rig is employed to generate a flow similar to the one encountered in a Francis turbine operating at 70% load [7]. At this regime, the vortex rope is well developed and generates large pressure pulsations. The runner blades thus act like a turbine near the hub and a pump near the shroud. A special acquisition system was designed and implemented to measure the runner speed of 920rpm, at a discharge of 30 l/s. The rotation direction is considered as positive direction. The Reynolds number based on the throat diameter and bulk velocity is 3.81×10^5. The jet slot is embedded on the runner crown as it can be seen in Fig. 1. Five cases with different momentum fluxes are studied

- (U_r, U_θ, U_z) = (0, 0, 5m/s) with Q_{jet}/Q = 0.027 (hereafter c1)
- (U_r, U_θ, U_z) = (0, -5m/s, 5m/s) with Q_{jet}/Q = 0.027 (hereafter c2)
- (U_r, U_θ, U_z) = (0, 0, 10m/s) with Q_{jet}/Q = 0.037(hereafter c3)
- (U_r, U_θ, U_z) = (0, -10m/s, 10m/s) with Q_{jet}/Q = 0.037 (hereafter c4)
- (U_r, U_θ, U_z) = (0, -15m/s, 15m/s) with Q_{jet}/Q = 0.053 (hereafter c5).

This is an active flow control while in the turbines, a flow can be bypassed from the spiral casing and injected through a needle-controlled through the slot. For this reason, a highly narrow patch is considered as the jet slot.

The calculations reported herein are made using the finite-volume method in the FOAM-extend-3.0 CFD code. The second-order central differencing scheme is used to discretize the diffusion terms. The blended numerical scheme is used for convective terms. The scheme is the combination of linear-upwind differencing in URANS region and a limited linear total variation diminishing (TVD) scheme with a conformance coefficient in LES region. The convection term in the LES region is interpolated by 15% linear-upwind differencing and 85% central differencing. The mesh configuration is the same as the base case except the jet slot as an extra patch and a finer resolution around it. Figure 1b shows the resolution used in this study with 16×10^6 cells. The maximum CFL number is 10 for the c1 and is 15 for the c5. The maximum CFL number occurs at the jet exit. The CFL number at the throat is around one and the mean CFL number is 0.02.

The parallel processing is done through MPI and domain decomposition. To achieve a near-optimal parallel load balancing, the computational meshes are subdivided into blocks of equal size, which are submitted to individual cores of an AMD Opteron 6220 Linux cluster. The mesh resolution is run on 16 nodes with 16 cores each. The time-step corresponds to 0.028 degrees of runner rotation.

The homogeneous Neumann, is applied at the outlet boundary for pressure and the turbulence quantities. The *inletOutlet* condition, which is a homogeneous Neumann condition with the limitation of no backflow, is applied at the outlet boundary for the velocity. A constant velocity is applied at the jet slot. The General Grid Interface (GGI) is used at the interfaces between the rotating and stationary regions.

3. Results and Discussion

The mean velocity field is determined by time averaging over five complete runner revolutions to filter out all unsteadiness. The survey axes, S^*, at sections W0-W2 (see Fig. 1), are normalized by the throat radius, R_{throat}=0.05m, and the velocity is normalized by the bulk velocity at the throat, U_{throat}. The axial axis is downward and the runner rotates in the positive direction.

Figure 2 shows the tangential and axial mean velocity for different flow configurations with and without flow control at W0-W2. There is not any major difference among velocity profiles at W0 where is very close to the jet slot. At W1 which is at the throat, the jet momentum flux plays an important role. There are two features that should be controlled to alleviate the pressure pulsation and remove the on-axis recirculation region. First, the swirl should be neutralized, i.e. the tangential velocity close to the hub and the runner crown should be controlled. Javadi et al. [8] studied the swirl generator at different runner rotational speeds and concluded that the size of the vortex rope, width of the on-axis recirculation region and the pressure pulsation are directly related with the swirl close to the hub. Second, the wake of the runner crown is also responsible for the on-axis stagnant region. A successful control technique should address both issues and be practical as well. The c1 only addresses the second issue but not sufficiently. It can be seen that c1 attempts to remove the wake of the crown. The pure axial nature of the c1 fails to neutralized the swirl and even increases it. The weakened wake of the crown and shortened on-axis recirculation region gives room to the high pressure flow region to expand and the tangential component of the velocity to increase, see Fig. 2b. This is the reason for increased swirl for the c1, c2 and c3 at W1. This increase for c2 is even stronger. The tangential component of c2 is not strong enough to alleviate the swirl, while it weakens the wake more than the c1 and c3.

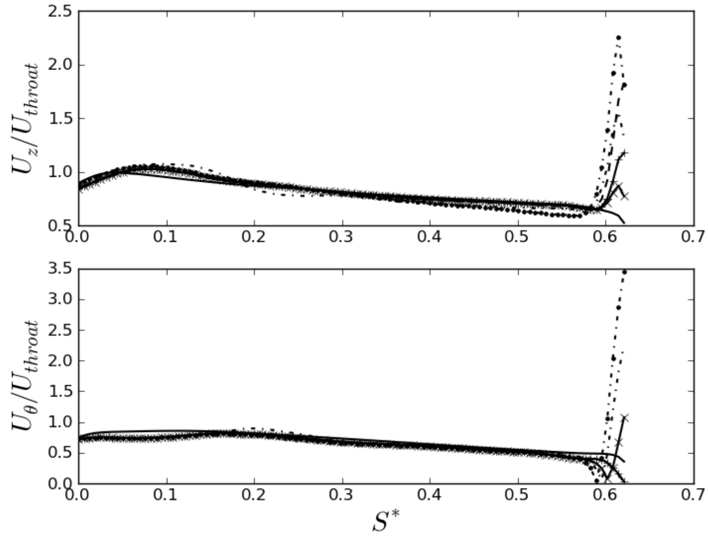

(a) W0

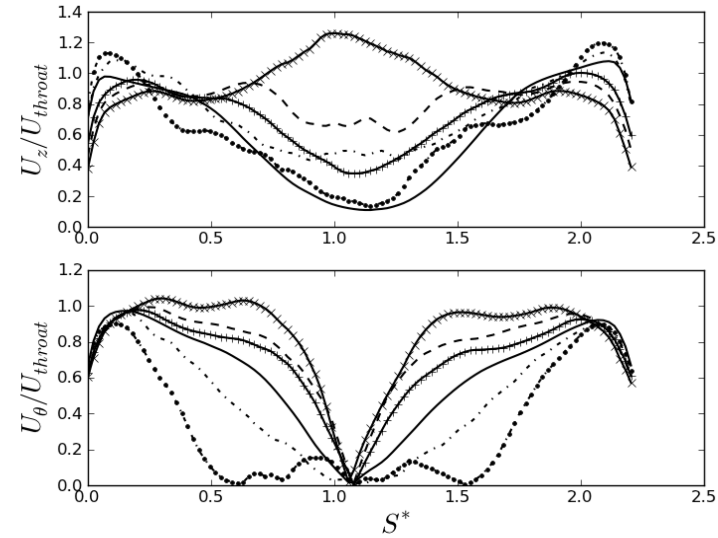

(b) W1

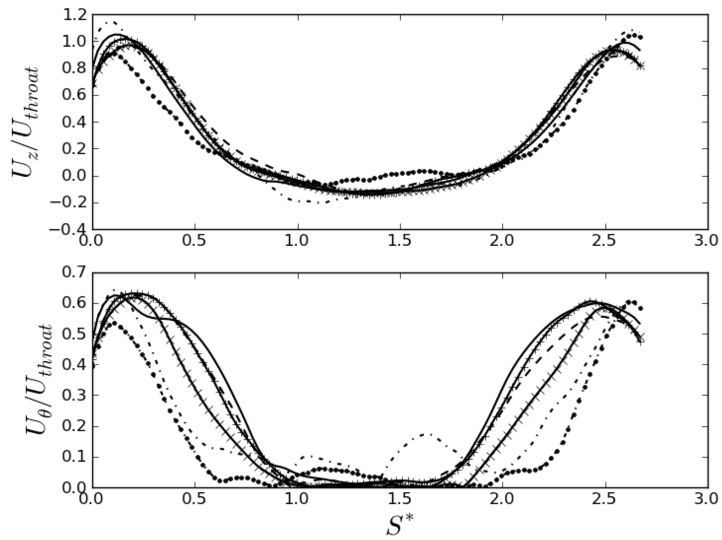

(c) W2

Fig. 2 Axial and tangential velocity. Solid: no jet. Solid with +: c1. Solid with ×: c2. Dash: c3. Dash dot: c4. Dot: c5

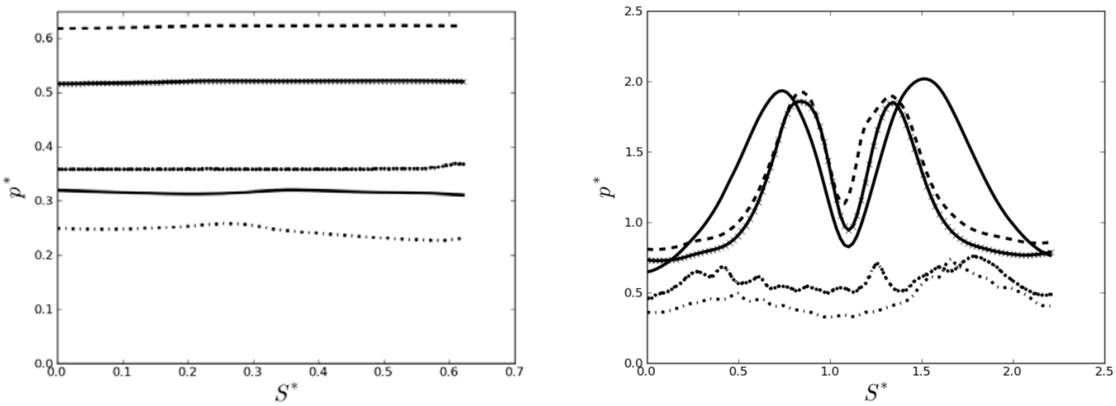

(a) W0 *(b) W1*

Fig. 3 Pressure fluctuation. Solid: no jet. Solid with ×: c2. Dash: c3. Dash dot: c4. Dot: c5

The tangential velocity increases linearly with the radius at W1 for the case with no jet, whereas the trend is nonlinear for the c1, c2 and c3. Since the swirl is not affected adequately for these three configurations, the on-axis stagnant region still remains at W2, see Fig. 2c. It can be seen that the c2 decreases the swirl more than the c1 and c3 due to its tangential component. Thus, a yawed jet with opposite direction relative to the runner rotation should be issued from the slot. The point about the first three jets is that all of them remain attached to the crown. The c4 and c5 separate from the crown at the mid way due to their stronger momentum fluxes compared with other first three jets, see Fig. 5. Although the separation from the crown helps them to penetrate further off-axis to alleviate the swirl more, they affect the wake of the crown less than other cases. Another issue is that if the jet detaches from the crown, as a wall-mounted bluff body, it creates its own wake. Figure 2b shows that both cases, the c4 and c5, affect the wake of the crown less than the c2, while they decrease the swirl more than other cases. The c5 decreases the swirl much more than other cases. However, the wake of the crown still forms an on-axis stagnant region, see Fig. 2c. Therefore, in order to remove the on-axis recirculation and stagnant regions, a jet should be applied to keep both benefits, remain attached to the crown and be strong enough to decrease the swirl, i.e. a jet with a strong tangential component and an adequate axial component. The optimized place of the injection slot is another way to avoid the separation.

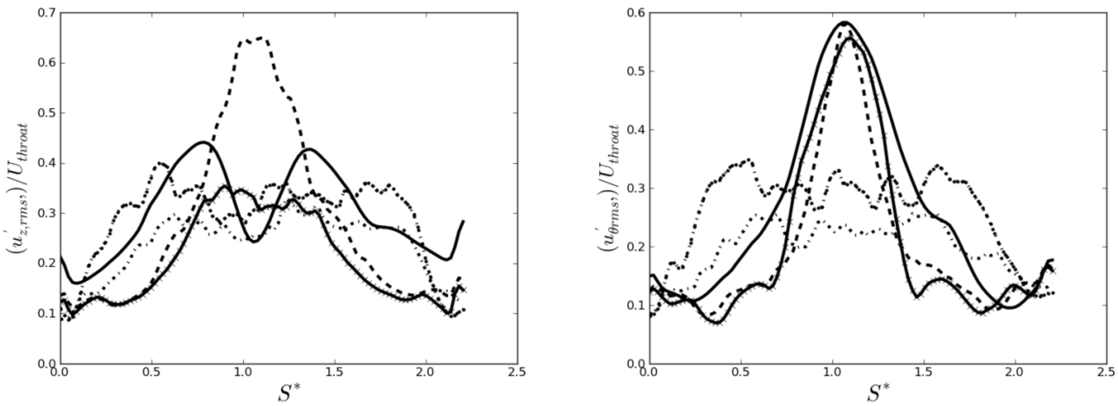

(a) axial *(b) tangential*

Fig. 4 Velocity fluctuations at W1. Solid: no jet. Solid with ×: c2. Dash: c3. Dash dot: c4. Dot: c5

Figure 3 shows the pressure fluctuation root mean square normalized by water density and U^2_{thraot}. It can be seen that the pressure pulsation increases at W0 for c2 and c3 while for c4 and c5 are at the same level as that in the case without jet control. At W1, since the c2 and c3 do not decrease the swirl, the pressure pulsations are very similar to that in the case without jet. The c4 and c5 are highly effective in decreasing the pressure pulsation at the throat.

Figure 4 shows the axial and tangential velocity fluctuation root mean square at W1 for all cases. Since the c2 and c3 do not decrease the swirl which is the main source of the on-axis recirculation region, they do not decrease the level of turbulence compared with the case without jet. It is worth mentioning that the pure axial nature of the c3 even increase the axial velocity fluctuation at W1 tremendously. As mentioned before, the c4 and c5 decrease the swirl and the shear between the on-axis recirculation region and the marginal region with strong axial velocity. Thus, they decrease the level of turbulence in the draft tube.

Figure 5 shows a snapshot of axial velocity in the draft tube for the c2 and c5. It can be seen that the jet separates from the crown in the c5 and fails to remove the wake of the crown. In contrast, the c2 removes the wake of the crown while the residual swirl creates an on-axis stagnant region in the downstream. However, both cases decrease the size of the vortex rope.

Figure 6 shows the iso-surface of *q*-criterion in the draft tube representing the effect of different jets on the vortex rope. The case without jet control presents the largest vortex rope and all cases with a jet injection presents a smaller one. It can be seen that the size of the vortex rope follows the same aforementioned pattern. The c4 and c5 remove the large scale coherent structure in the draft tube and instead generate lots of smaller on-axis structures only around the throat. In the other words, in the absence of strong pressure pulsation and turbulence, the remained on-axis stagnation region at W2 can be completely removed by a small modification.

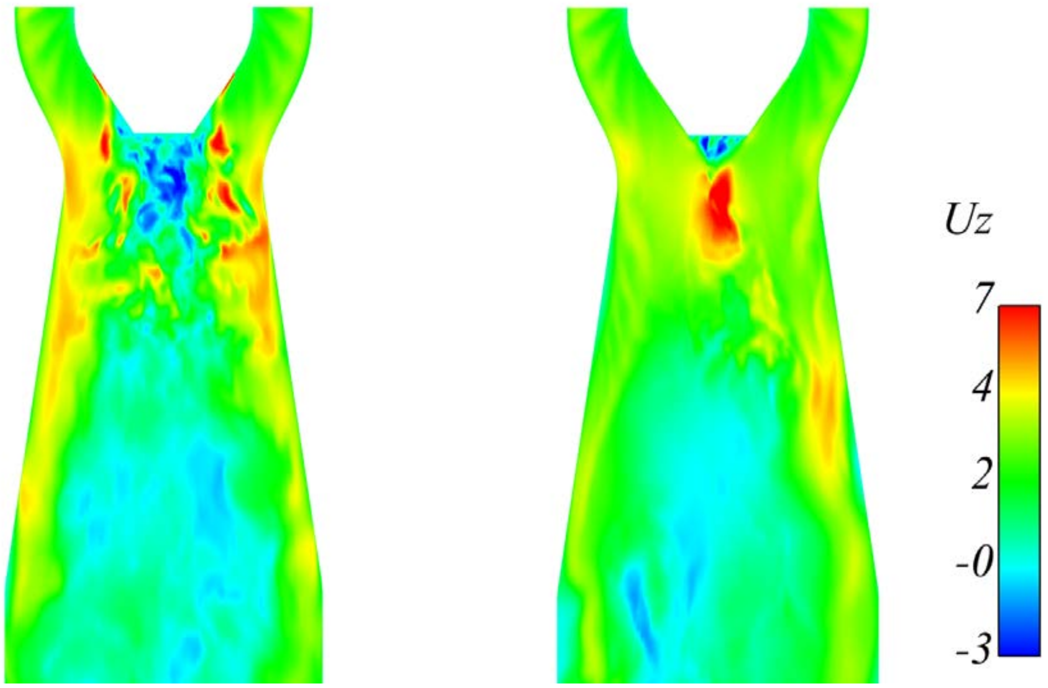

(a) c5 *(b) c2*

Fig. 5 Instantaneous axial velocity

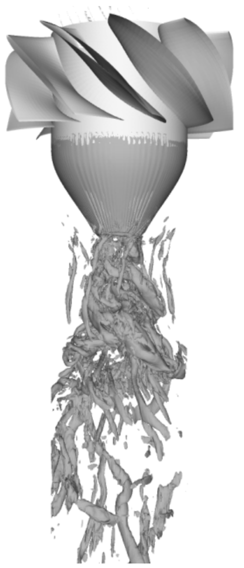

(a) no jet

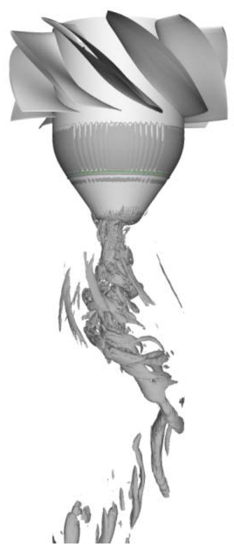

(b) c1

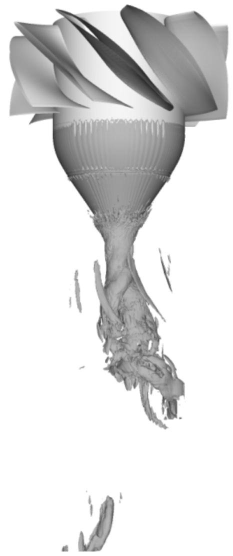

(c) c2

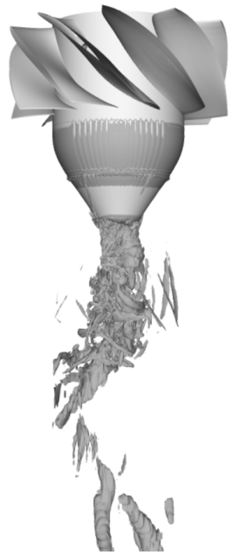

(d) c3

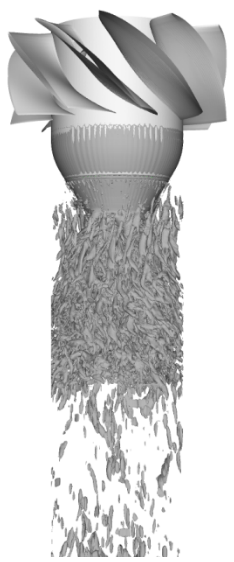

(e) c4

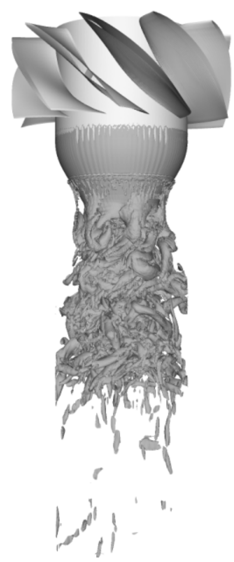

(f) c5

Fig. 6 q-criterion in draft tube for different flow configurations

4. CONCLUSION

The vortex rope similar to the one occurs in the Francis turbine part-load is controlled using a jet injection from the runner crown. Five different cases with different momentum fluxes are studied. The c1, c2, and c3 are not strong enough to decrease the swirl in the draft tube although they remove the wake of the runner crown. The c4 and c5 are strong enough to decrease the swirl in the draft tube, whereas they separates from the crown and fails to remove the wake of the runner. The c4 only needs 4% of total volume flux of the swirl generator. Although this method is practical and easy to install, the place of the injection and the momentum flux are important factors in the applicability of the technique.

5. ACKNOWLEDGEMENTS

The research presented was carried out as a part of the "Swedish Hydropower Centre- SVC". SVC is established by the Swedish Energy Agency, EnergiForsk and Svenska Kraftnät together with Luleå University of Technology, The Royal Institute of Technology, Chalmers University of Technology and Uppsala University, www.svc.nu. The computational facilities are provided by C3SE, the center for scientific and technical computing at Chalmers University of Technology, and SNIC, the Swedish National Infrastructure for Computing.

6. REFERENCES

[1] Javadi A. and Nilsson H.: Time-accurate numerical simulations of swirling flow with rotor-stator interaction. *J. Flow, Turbulence and Combustion.*2015 (in press).

[2] Kjeldsen M., Olsen K.M., Nielsen T. and Dahlhaug O.G.: Water injection for the mitigation of draft-tube pressure pulsations. *IAHR International Meeting of W.G. on Cavitation and Dynamic Problems in Hydraulic Machinery and Systems.* Barcelona, Spain. 2006.

[3] Susan-Resiga R., Muntean S., Hasmatuchi V., Anton I. and Avellan F.: Analysis and prevention of vortex breakdown in the simplified discharge cone of a Francis turbine. *ASME J. Fluids Eng* .Vol. 132. 2010. 051102-1.

[4] Tănasă C., Bosioc A., Muntean S. and Susan-Resiga R.: Flow-feedback method for mitigating the vortex rope in decelerated swirling flows. *ASME J. Fluids Eng.* Vol. 135(6). 2013. pp. 1-11.

[5] Javadi A. and Nilsson H.: LES and DES of strongly swirling turbulent flow through a suddenly expanding circular pipe. *Comput. Fluids. Vol.*107. 2015. pp. 301-313.

[6] Javadi A. and Nilsson H.: LES and DES of swirling flow with rotor-stator interaction. *Progress in hybrid RANS-LES modelling.* Vol.130. 2014. pp. 457-468.

[7] Resiga, R., Muntean S., Bosioc, A.I., Stuparu, A., Milos, T. and Baya, T.: Swirling flow appratus and test rig for ow control in hydraulic turbines discharge cone. *2nd IAHR International Meeting of the Workgroup on Cavitation and Dynamic Problems in Hydraulic Machinery and Systems, Timisoara, Romania.* 2007.

[8] Javadi, A., Bosioc, A., Nilsson, H., Muntean, S. and Resiga, R.: Velocity and pressure fluctuations induced by the precessing helical vortex in a conical diffuser. *IOP Conf. Ser.: Earth Environ. Sci.* Vol. 22. 2014. 032009.